Scientific Research Publishing

Journal of Geoscience and Environment Protection, 2022, 10, 234-252
https://www.scirp.org/journal/gep
ISSN Online: 2327-4344
ISSN Print: 2327-4336

Mapping of Malaria Risk Related to Climatic and Environmental Factors by Multicriteria Analysis in the Marahoué Region of Côte d'Ivoire

Assikohon Pulchérie Gouzile[1*], Martial Bama[1], Bi Yourou Guillaume Zamina[1], Ellélé Aimé Yapi[2], Gneneyougo Emile Soro[3], Bi Tie Albert Goula[3], Tiembré Issiaka[1,2]

[1]National Institute of Public Hygiene, Abidjan, Côte d'Ivoire
[2]Félix Houphouët Boigny University, Abidjan, Côte d'Ivoire
[3]Nangui-Abrogoua University, Abidjan, Côte d'Ivoire
Email: *gouzilepul@yahoo.fr

How to cite this paper: Gouzile, A. P., Bama, M., Zamina, B. Y. G., Yapi, E. A., Soro, G. E., Goula, B. T. A. and Issiaka, T. (2022). Mapping of Malaria Risk Related to Climatic and Environmental Factors by Multicriteria Analysis in the Marahoué Region of Côte d'Ivoire. *Journal of Geoscience and Environment Protection, 10,* 234-252.
https://doi.org/10.4236/gep.2022.106015

Received: March 19, 2022
Accepted: June 27, 2022
Published: June 30, 2022

Abstract

Malaria, a febrile human disease transmitted by female anopheles whose ecology is linked to water, is a major public health problem in Côte d'Ivoire, more precisely in the Marahoué region located in the southwest of the country. In order to effectively control this disease, it is necessary to understand the etiology and the diffusion pattern of the vectors. This justifies this study, which proposes to determine the areas at risk of malaria transmission in order to carry out an effective fight against this disease in this region of Côte d'Ivoire. To achieve this, a combined approach of geographic information systems and multicriteria analysis was adopted. The analysis reveals that the south and northwest of the Marahoué region present a high risk for malaria transmission. This risk is linked to indicators such as climatic factors that cover 48.36% of the study area, environmental factors such as vegetation cover (NDVI), soil moisture (NDWI), altitude, hydrography (water point) and population that covers 55.29% of the area and land use. Also, the results indicated that 50.70% of the region has favorable conditions for malaria transmission. Overall, climatic and environmental indicators are the risk factors associated with the resurgence of malaria.

Keywords

Mapping, Palustrum, Multicriteria Analysis, Marahoué, Ivory Coast

1. Introduction

Malaria is one of the major public health problems. According to the latest WHO report on malaria in the world, 241 million cases were reported in 2020 with 627,000 deaths (WHO, 2021). The most affected region is sub-Saharan Africa with 96% of deaths, 80% of which are in children under five (WHO, 2021). Climate plays an important role in the dynamics and distribution of malaria (Gouataine & Ymba, 2018; Fosah et al., 2022). Variations in climatic conditions, such as temperature, rainfall patterns, and humidity have a significant effect on vector life span, parasite development, and subsequently disease transmission (Diomandé et al., 2017; Fosah et al., 2022; Zewga, 2021). Furthermore, the risk of transmission increases in a poorly maintained environment characterized by the proliferation of illegal dumpsites, the discharge of wastewater in the streets, and the presence of stagnant water after rainfall. Stagnant water provides potential breeding grounds for the malaria vector (Gramado et al., 2006; Gouataine & Ymba, 2018).

Côte d'Ivoire is a malaria endemic country (Eholié et al., 2004; Konan et al., 2009). More than 80% of general consultations in the Etablissements Sanitaires de Premiers Contacte (ESPC) are attributed to malaria (PNLP, 2005). The major vector in this country is *Anopheles gambiae* (PNLP, 2005). The Marahoué region, located in the central-western part of Côte d'Ivoire, presents favorable conditions for the development of many species of mosquitoes (excessive dumping of household waste, collection of wastewater due to the failure of the sanitation system, presence of shallows and ponds on sunny surfaces with the presence of vegetation). Despite the efforts put in place by the country, with the National Malaria Control Program (PNLP) created in 1996 and the adaptation of the National Strategic Plan (PSN) in 2016, this pathology remains endemic throughout the country with an incidence of 230‰ (PNS 2016-2020). In the Marahoué region, the incidence is 222.78‰ (RASS, 2018). This finding seems to indicate that the malaria control strategy does not exist sufficiently on the environmental health risk. This justifies this study whose objective is to determine the malaria risk areas for a more effective control of this disease in the Marahoué region of Côte d'Ivoire. The interest of this work is to provide results that will be used to solve health problems in which climatic and environmental factors intervene as factors favoring diseases and their vectors. Indeed, some tools such as mapping, remote sensing and geographic information systems are used to better target populations and areas at risk (Somé, 2010; Kotchi et al., 2019). Their studies respectively (Oluwafemi et al., 2022; Kouame et al., 2017) used multi-criteria analysis modeling and Geographic Information Systems (GIS) to map areas at risk to the Yellow Fever epidemic in Nigeria and the Acute Respiratory Infection in Côte d'Ivoire. Thus, this approach is best suited for assessing environmental health risk by combining epidemiological, statistical, and Geographic Information Systems (GIS) methods (Beale et al., 2008; Zewga, 2021).

2. Study Area

The Marahoué region is located in the central west of Côte d'Ivoire and straddles the forest zone and the savannah zone. This region includes three departments, Bouaflé, Sinfra and Zuénoula, and eleven (11) sub-prefectures, the largest of which are Bouaflé, Bonon, Gohitafla, Sinfra, Zaguiéta, and Zuénoula (Figure 1). According to the 2014 General Census of Population and Housing (RGPH), the population of the Marahoué region is estimated at 862,344 inhabitants, including 409,683 for the department of Bouaflé, 238,015 for the department of Sinfra, and 214,646 for the department of Zuénoula, with an average density of 94.57 hbts/km^2. The climate is equatorial and transitional, with an annual rainfall of 1800 mm. The climate has four seasons: a long rainy season from mid-March to mid-July characterized by abundant and frequent rainfall, followed by the short dry season from mid-July to mid-September, characterized by a quantitative decrease in rainfall. The short rainy season from (mid-September to November) is characterized by slow cumuliform cloud formations. The long dry season from November to mid-March is characterized by frequent morning fog. The Marahoué region is largely drained by the Marahoué River and Lake Kossou.

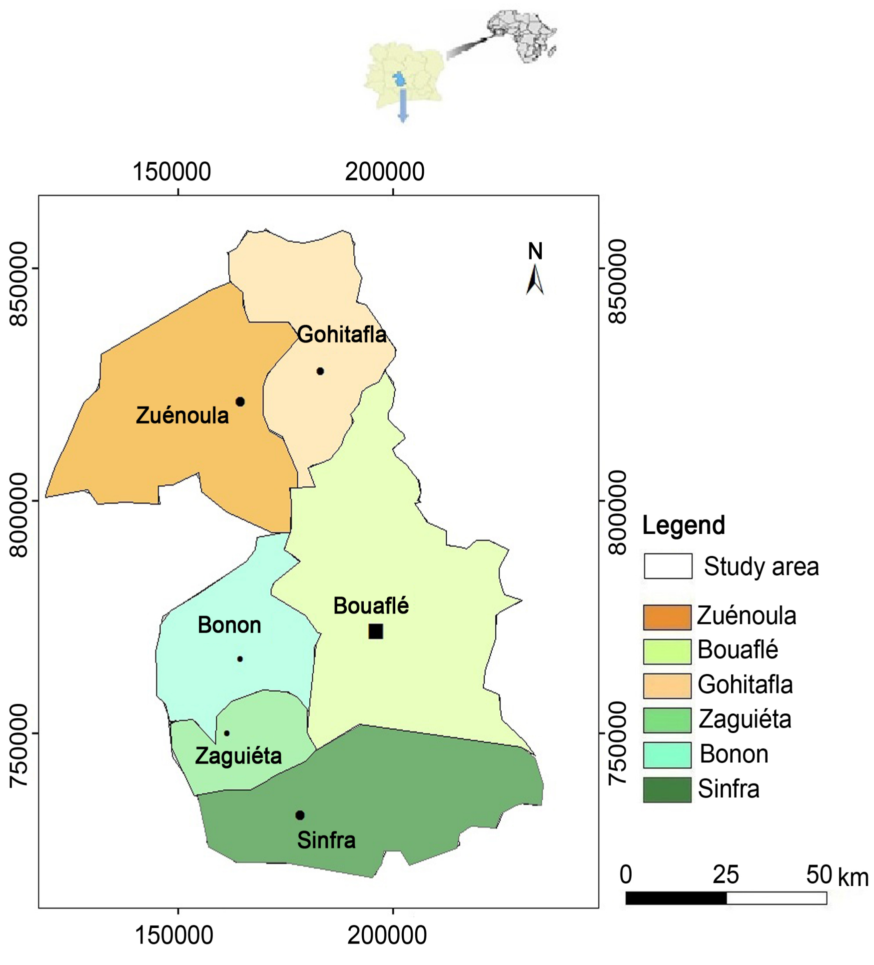

Figure 1. Presentation of the study area.

3. Materials and Methods

3.1. Materials

3.1.1. Climatic Data

The climatic data come from two sources made available to us by the National Meteorological Department, namely the Société d'Exploitation et de Développement Aéroportuaire, Aéronautique et Météorologique de Côte d'Ivoire (SODEXAM). They concern rainfall, minimum temperatures (min), maximum temperatures (max) and relative humidity. The first source concerns maximum and minimum temperature and relative humidity data from Daloa and Yamoussoukro, which are the closest synoptic stations to the region, as well as rainfall data from Bouaflé and Sinfra. The second source of rainfall, temperature and relative humidity data from the Zuénoula agro-climatic station was provided by the SUCAF sugar complex in Zuénoula. Thus, the study area is covered by a network of three rainfall stations, two synoptic stations and one agro-climatological station with a study time window of 1980 to 2013. These data are estimated to assess the risk related to climatic factors. The characteristics of the stations are recorded in **Table 1**.

3.1.2. Data

These data are composed of Landsat7 ETM+ (Enhancement Thematic Mapper plus) images at 30 m spatial resolution, Scene 197/055 acquired on December 12, 2003. These images were used to develop the land cover, vegetation index (NDVI) and soil moisture index (NDWI) maps.

The Schuttle Radar Topography Mission (SRTM) 3 digital elevation model (DEM) with a resolution of 30 m was used to produce the elevation map and the hydrographic network map. These data are estimated to assess the risk from environmental factors. The characteristics of the ETM images are presented in **Table 2**.

3.1.3. Population Data

The population data comes from the 2014 general population and housing census. This is data on human populations of communes and villages in the Ivory Coast. For this study, we used estimated 2018 data provided by the Direction de

Table 1. Climatological stations selected for the study.

Name	Station	Latitude North	Longitude West	Altitude (m)	Period
Bouaflé	Rainfall	9˚31	6˚28	421	1980-2013
Sinfra	Rainfall	9˚30	7˚34	434	1980-2013
Zuénoula	Rainfall	10˚29	6˚24	356	1980-2013
Daloa	Synoptic	6˚52	6˚28	276	1980-2013
Zuénoula	Agro-climatological	7˚25	6˚30	209	1980-2013
Yamoussoukro	Synoptic	6˚54	5˚21	196	1980-2013

Table 2. Spectral characteristics of Landsat7-ETM+.

Sensors	Spatial resolution	Number of bands	Path/Row	Date of acquisition	Producer
L4-5TM	30 m × 30 m	8	197/55	22/12/2003	USGS
LsoLi	30 m × 30 m	8	197/55	22/12/2003	USGS

l'Information de la Planification et de l'Evaluation (DIPE).

3.2. Tools

The data processing required the use of the following software:

ArcGis 10.2 for mapping risk areas using inverse distance weighted interpolation (IDW);

Envi 4.7 from RSI (Research System Incorporation) was used to process the acquired images and land cover.

3.3. Methodology

The mapping of areas at risk of malaria proliferation was done by the Multicriteria Analysis of Saaty (1977). Mapping areas of potential malaria risk requires climatic, environmental, and land use data. These data are the factors that favor malaria transmission and the proliferation of malaria mosquito breeding sites (Guerra et al., 2008; Gething et al., 2011). Studies (Hay et al., 2009; Ferrão et al., 2021) have used mean temperature sometimes with precipitation and/or humidity to develop maps representing spatiotemporal variation in malaria transmission risk. The approach consists of classification and standardization of criteria, weighting of criteria and aggregation following the multi-criteria approach (Jourda et al., 2006; Koudou et al., 2013).

3.3.1. Choice of Decision Criteria

The criteria used to characterize potential malaria transmission risk areas include climatic factors such as rainfall, maximum and minimum temperatures, and relative humidity; environmental and/or ecological factors such as vegetation cover, soil moisture, altitude, standing water, garbage dumps, irrigated and drained areas, and densely populated areas. The female Anopheles mosquito vector proliferates in an insoluble environment characterized by the presence of stagnant water, vegetation cover and garbage dumps. Rainfall is important because it favors the development of the vectors by providing them with suitable habitats to reproduce. After rainfall, the presence of stagnant water provides potential breeding sites for the female Anopheles mosquito. Temperature is a key factor for many mosquitoes and for the life of the parasite in the mosquito. Thus, the factors favoring the risk of malaria transmission include three indicators: climatic vulnerability, environmental vulnerability and land use.

1) Climate vulnerability

The climatic vulnerability indicator reflects the set of climatic factors that favor the presence of malaria. It results from the linear combination of the maps of precipitation, maximum and minimum temperature and relative humidity obtained by the Inverse Distance Weigthing (IDW) interpolation technique of the ArcGIS.10.2 geostatitica analyst extension.

2) Environmental vulnerability

The environmental vulnerability indicator translates environmental and/or ecological factors resulting from the linear combination of the vegetation index map (NDVI), soil moisture index (NDWI), altitude, distance to any water point (hydrography) and the population density map. It thus conditions the environmental factors that favor the development of germs and/or vectors.

Vegetation index or Normalized Difference Vegetation Index (NDVI) and Soil Moisture Index or Normalized Difference Water Index (NDWI) maps are obtained from Landsat ETM+ image processing by color composition using ENVI 4.7 software. The study area was extracted by binary mask on a Landsat 7 scene. The vegetation index was determined by the "weighted difference" formula. If the vegetation cover is dense and chlorophyll active, the index tends towards 1. However, when the index is low, the less vegetation there is. The formula for calculating this index is:

$$\text{NDVI} = \frac{\text{PIR} - \text{R}}{\text{PIR} + \text{R}} \tag{1}$$

With PIR the near infrared and R the Red. In the case of the Landsat ETM+ images that we used, the PIR corresponds to the ETM+3 band and R to the ETM+4 band. In addition, the soil moisture index is obtained by the following formula

$$\text{NDWI} = \frac{\text{TM4} - \text{TM5}}{\text{TM4} + \text{TM5}} = \frac{\text{PIR} - \text{MIR}}{\text{PIR} + \text{MIR}} \tag{2}$$

Hydrography and elevation are obtained from the Schuttle Radar Topography Mission (SRTM3) Digital Elevation Model (DEM) and the population density map is obtained by the Inverse Distance Weigthing (IDW) interpolation method, from the ArcGIS.10 geostatitica analyst extension. Population density values result from the ratio of population to area of each locality in the region.

3) Land use

Like vegetation and soil moisture, land cover is obtained from Landsat ETM+ image processing by color compositing on ENVI 4.7. The extraction of the study area is performed by binary mask on a Landsat 7 scene. The colored composition consists in displaying simultaneously on the screen three image bands in the basic channels (Red/Green/Blue) and facilitates the extraction of information. In this study, the color composition of Landsat EM and ETM+ bands 7-5-6 was used because it presents the best land cover type discrimination.

3.3.2. Classifications and Standardization of Decision Criteria

The identified decision criteria were subdivided into different classes representing either a particular environment or a confidence interval. Two classes labeled low and high risk were retained for each criterion for better interpretation (Kouamé et al., 2011). Subsequently, the different classes for each criterion were standardized according to their particular influence on the disease. These classes were coded (numerical coding). The results of the combinations of the two classes of the different factors are also grouped into two classes ranging from low to high risk. The different criteria are then combined into indicators. These are in turn "divided" into two classes (low risk and high risk) and coded. It is ultimately the combination of the indicators that gives the overall malaria risk maps. The classes obtained for each of the criteria, and the codes assigned to them, are shown in **Table 3**.

3.3.3. Weighting of Criteria

The decision criteria are weighted according to the linear combination method based on the pairwise comparison technique according to the Analytic Hierarchy Process (AHP) of Saaty (1977). It is developed by Meyer-Waarden, L. & Zeitoun, H. (2005) and used by Koudou et al. (2013) and Yao et al. (2014). This method generates standardized weights whose sum is equal to 1. It first consists of a binary comparison of the relative importance of all elements belonging to the same hierarchical level with respect to the element of the next higher level according to the numerical scale proposed by Saaty (**Table 4**). Then, set up a reciprocal square matrix formed by the evaluations of the ratios of the weights ($K \times K$), K being the number of elements compared. In this way we obtain:

Table 3. Classification and standardization of decision criteria.

Criteria	Parameters	Values	Ribs	Classes
Plant cover	ndvi	<−0.02 and >0.41	1	low risk
		from −0.02 to 0.41	2	high risk
soil moisture	ndwi	<−0.2 and >0.94	1	low risk
		from −0.2 to 0.94	2	high risk
Hydrography	distance at any point	>1.5 km	1	low risk
		<1.5 km	2	high risk
relief	altitude	>137 m	1	low risk
		<137 m	2	high risk
Population	population density	<98.08	1	low risk
		>98.09	2	high risk
precipitation	Annual rainfall	<1174 and >1275	1	low risk
		1174 à 1275	2	high risk
Temperature	Temperature value	<20.8 and >32.30	1	low risk
		20.8 à 32.30	2	high risk
Relative humidity	Humidity level	>78.06	1	low risk
		<78.06	2	high risk

Table 4. Verbal and numerical expression of the relative importance of criteria (El Morjani, 2003).

Expression of one criterion in relation to another	Note
Same importance	1
Moderately important	3
Highly important	5
Very important	7
Extremely important	9
Extremely less important	1/3
Significantly less important	1/5
Less important	1/7
Extremely less important	1/9

$$a_{ji} = \frac{1}{a_{ij}} \quad (3)$$

With $a = a_{ij}$ and $a_{ij} = 1$ (reciprocal value) where a is the value of each factor i and j are the rows and columns respectively (Saaty, 1977). Finally, the linear combination method is used to determine the weights of each criterion by the approximate method of computing eigenvectors (Vp_i). The eigenvectors are obtained by calculating their geometric means per row. The Vp_i is determined by the following formula:

$$V\rho_i = \sqrt[n]{\prod_{i=1}^{n} N_i} \quad (4)$$

$$W_i = \frac{V\rho_i}{\sum_{i=1}^{n} V\rho_i} \quad (5)$$

With: $V\rho_i$ eigenvector of each criterion, N_i value of each criterion. The weighting coefficient W_i is determined as follows

The binary comparison matrix and criteria weights for each criterion and for the three indicators are reported in Table 5.

3.3.4. Evaluation of the Decision Criteria

Various methods are applied for the evaluation of decision criteria in multicriteria analysis. In this study, to evaluate the decision criteria, the full aggregation method by weighting used by Joperin (1995) and Saley (2003) was implemented. It consists of multiplying each criterion or indicator by its weighting coefficient and then adding the results to produce a fitness index according to the following equation:

$$S = \sum_{i=1}^{n} w_i x_i \quad (6)$$

With: S the final result; W_i: the weight of the criteria i; X_i; standardized value of the criterion i.

This method was used for the climate vulnerability and environmental indicators.

Table 5. Weighting of risk factors for malaria.

Parameters	Eigenvector (EV)	Coefficient of weighting (CP)
Rain	2.6	0.51
Maximum temperature	1.3	0.26
Minimum temperature	0.4	0.08
Relative humidity	0.8	0.15
Climatic factors	**2.47**	**0.64**
NDWI	2.67	0.43
NDVI	1.55	0.25
Population	0.64	0.10
Altitude	0.37	0.06
Distance to water sources	1	0.16
Environmental factors	**1**	**0.26**
Land use	**0.41**	**0.10**

The realization of the "malaria risk" map consists in transferring in space the different values resulting from the addition of the standardized and weighted values of each indicator added to the land use. A reclassification of the factors allowed the realization of thematic maps with two classes expressed in risk, namely low risk and high risk. The number of classes is fixed at two for a better readability and a good interpretation of the map.

3.3.5. Map Validation Method

The validation of the maps consists in the analysis of the uncertainty and error of the maps. The analysis consists of calculating the uncertainties of the average of the different parameters of the main indicators of power and vulnerability. The uncertainty is calculated by the following equation:

$$\Delta\overline{X} = \frac{\sigma}{\sqrt{m}} \tag{7}$$

With: Δx: the uncertainty of the mean of the data series; σ: the standard deviation of the data series; m: the number of data.

To determine the confidence interval, an expansion factor (K) is then calculated. The determination of this factor is based on the principle of statistical calculation of the expanded uncertainty. The K factor allows the definition of an interval of sufficient range to have a high confidence in the results. The expression of this factor is as follows:

$$K = \frac{\left|E - \overline{X}\right|}{\sigma} \tag{8}$$

With: K: expansion factor; E: extreme value of the statistical series. It can be the maximum or minimum of the series; σ: standard deviation of the series.

The confidence level of the different parameters was deduced from the different values of K. Thus, $K = 1$ for the 68% confidence level, $K = 2$ for the 95% confidence level, and $K = 3$ for the 99% confidence level (Yao et al., 2014).

4. Results

4.1. Land Use

The land use map shows five landscape classes, which are dense forest, degraded forest, crops (fallow), water, and bare soil and habitats. The main classes are dense forest, degraded forest and crops/fallow. Dense forest appears as a support in which the other classes are embedded.

The dense forest is observed practically throughout the study area at various points. However, it is more present in the west of the study area, precisely at the level of the park of Marahoué. It occupies 44.8% of the total area. Degraded forest, crops and fallow land, bare soil and water occupy 22.7%, 22.90%, 9.1% and 0.5% of the total area, respectively (**Figure 2**). This dense forest has practically disappeared due to various human activities. These include deforestation for agriculture (presence of crops/fallow) and land use planning with the progress of urbanization through the policy of decentralization. This disappearance of the forest could also be due to the decrease in rainfall in this region. In the southern part of the region, the presence of degraded forest is noted.

4.2. Malaria Risk Related to Climatic Factors

The malaria risk according to climatic factors is represented in **Figure 3**. The

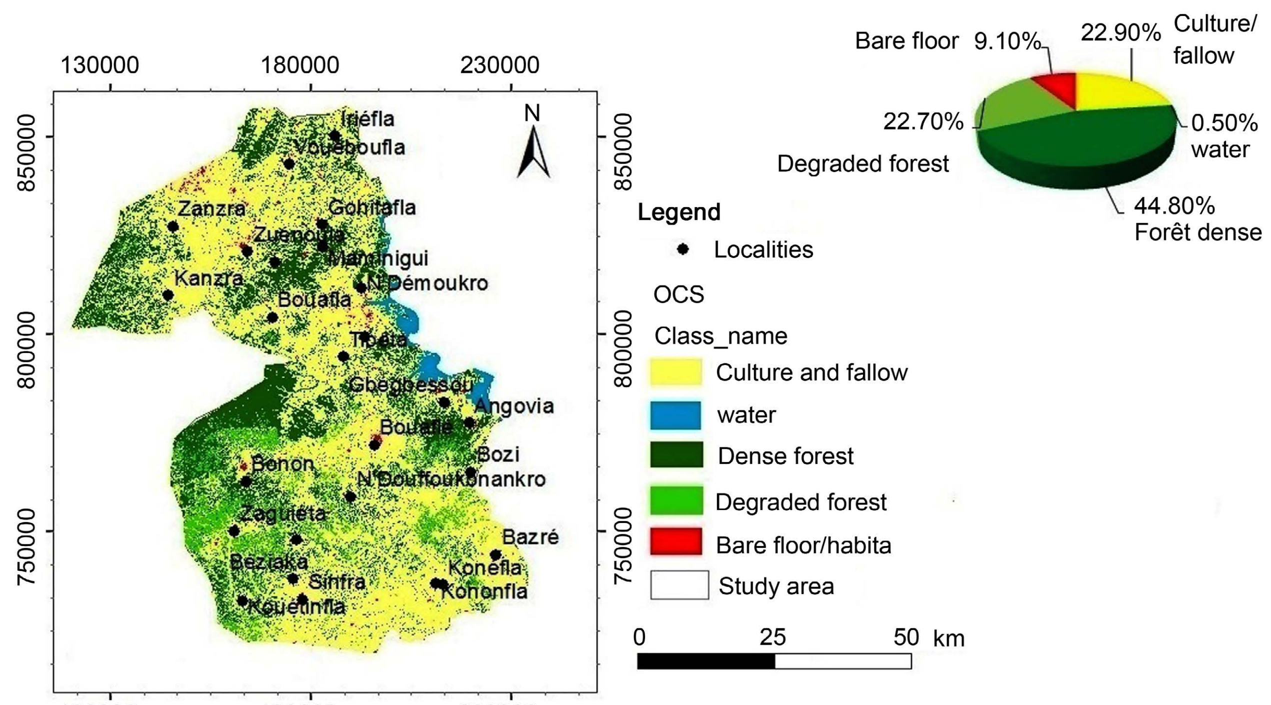

Figure 2. Land use map of the Marahoué region.

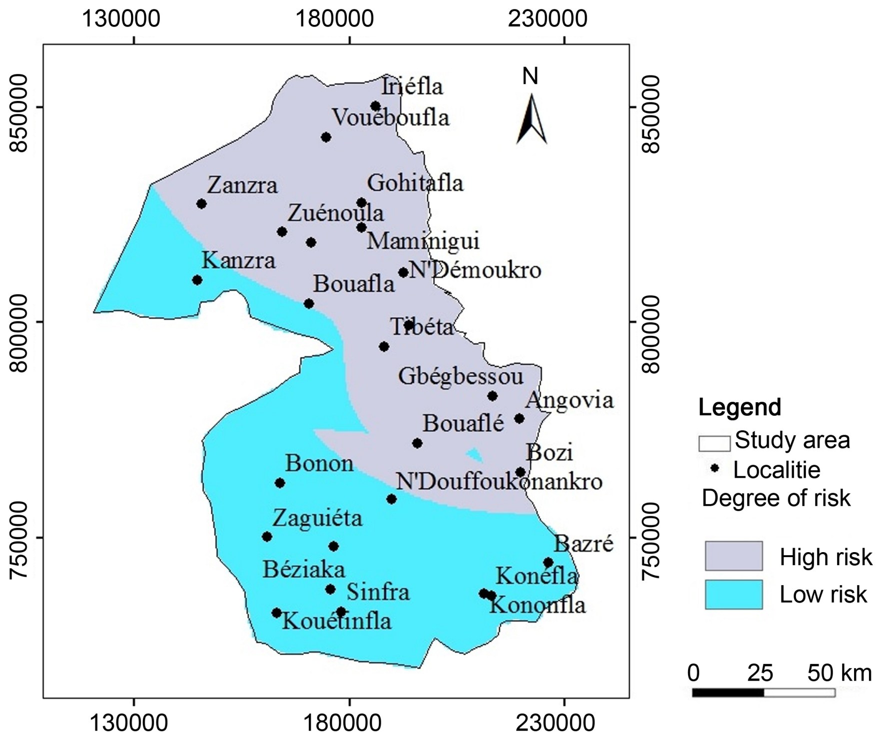

Figure 3. Malaria risk map related to climatic factors.

analysis of the map shows two classes:

- The low risk class is located in the north and central-east of the study area and is characterized by low rainfall of less than 1152 mm, very high maximum temperatures (35˚C) and high relative humidity (>60%). This risk represents 51.64% of the total area and occupies almost all of the Zuénoula health district and part of the Bouaflé district. These temperatures limit the sporogonic development of *plasmodium falciparum* in the mosquito and therefore do not favor malaria transmission.
- The high risk class covers 48.36% of the total area of the study area. This zone extends from the extreme northwest through the central west of the region to the south. It also affects the Marahoué National Park and is characterized by abundant rainfall, high maximum temperatures (30˚C) and very high relative humidity (>75%). This risk is limited to the Sinfra health district and certain localities in Bouaflé and Zuénoula. Rainfall favors the presence of watering holes and perennial ponds, which constitute mosquito breeding grounds. The temperature favors the reproduction of the vector. These factors present favorable conditions for the proliferation of the vector, the maturity of the parasite and the transmission of the disease.

4.3. Malaria Risk Related to Environmental and/or Ecological Factors

The risk due to environmental factors reflects the vulnerability of malaria due to variables such as vegetation cover, soil moisture, distance to water points (hydrology), altitude and population density. Mosquitoes, the vectors of malaria, and *Plasmodium falciparum* thrive in these factors. Figure 4 presents the malaria risk map according to environmental and/or ecological parameters. This map is identified in two classes of degree of risk.

- The low risk class is located in the north of the region and in certain localities of Bouaflé (Tibiéta, Bouafla.). It covers 44.71% of the region and is characterized by a degradation of the vegetation cover, a low soil moisture level due to low rainfall, and high altitudes. These factors reflect the low transmission of the disease. However, some endemic areas (Zuénoula) can be detected because of environmental conditions characterized by the presence of domestic wastewater due to the failure of the sanitation network (lack of proper piping), and household waste deposits (Photo 1).
- High risk covers more than half of the region (55.29%) and is located in the south of the region, specifically in the departments of Sinfra and Bouaflé, in the area of the Marahoué National Park and near Lake Kossou. This area is characterized by the presence of water points, low altitudes and a high population density. The vegetation cover is dense, resulting in soil moisture. This zone is characterized by the presence of large cities in the region and is confronted with a sanitation problem with the presence of garbage dumping at every turn (Photo 1).

4.4. Global Malaria Risk Mapping

The overall malaria risk map is derived from the linear combination of the climate, environmental, and land use risk maps according to their respective weights (Figure 5).

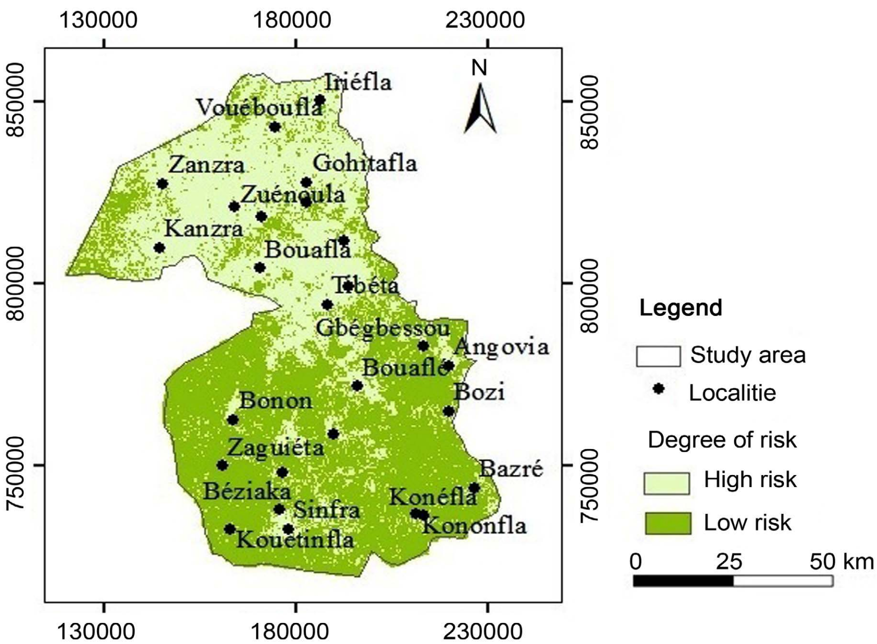

Figure 4. Malaria risk map by environmental factors.

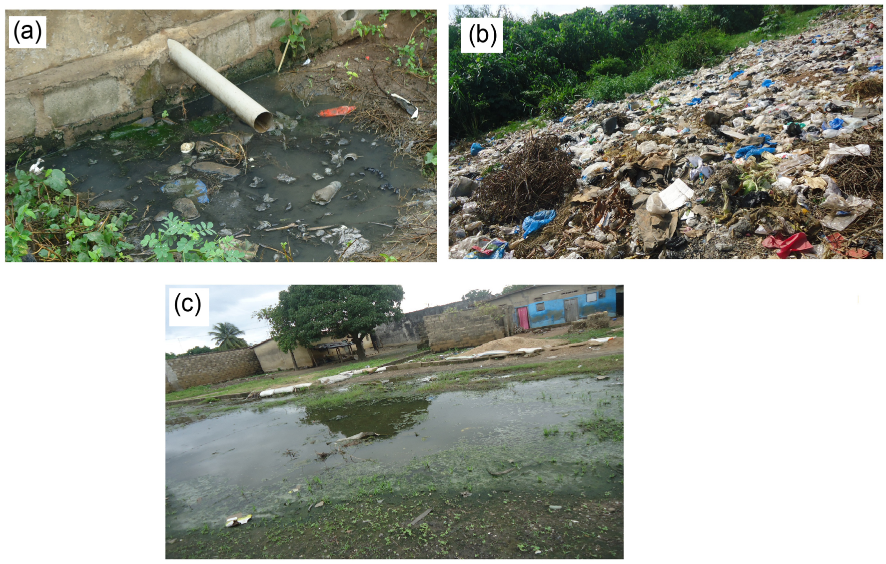

Photo 1. Proliferation area of the *Anopheles* vector of malaria in the Marahoué region (a) Wastewater (b) Household garbage dump and (c) Puddle.

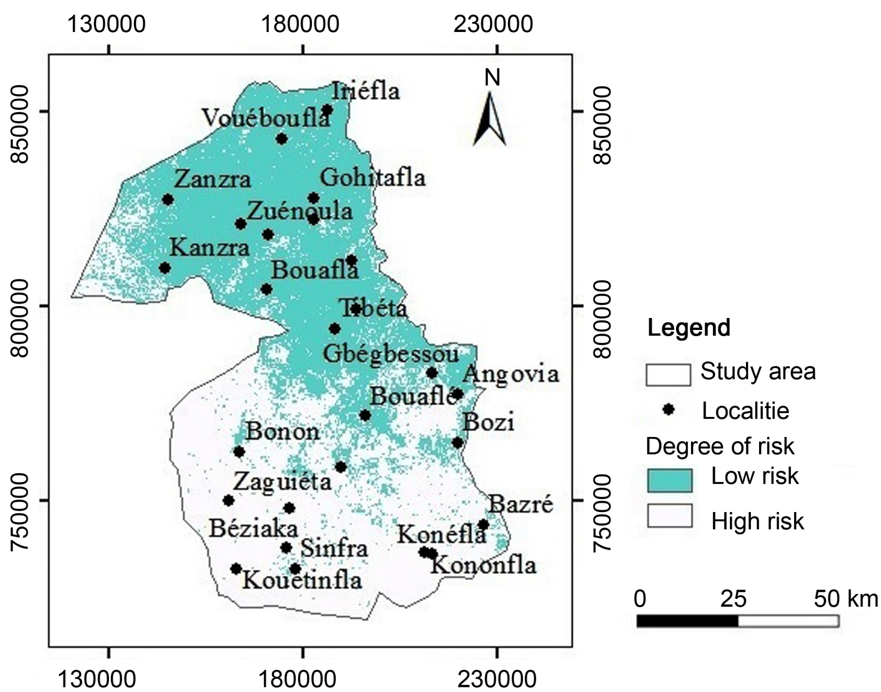

Figure 5. Global malaria risk map.

Observation of the map shows that the southern and northwestern parts of the region are more vulnerable to malaria transmission with a high risk level of 50.70%. Located in the pre-forest part of the region, these areas are characterized by abundant rainfall favoring the presence of stagnant water points which constitute the places of proliferation of the mosquito, temperatures between 21 and 30˚C leading to the virulence, aggressiveness and infestivity of the vector (the mosquito) of malaria and the presence of vegetation and water points leading to

Table 6. Statistics of risk factor assessment criteria.

Parameters	max	min	average	Standard deviation	Total	Uncertainty	K	NC
Land use	5	1	4.07	1.32	21,760,440	0.0003	1	68
Climate sensitivity	4.35	2.52	3.2	0.48	39,716	0.002	2	95
Ecological sensitivity	4.8	1	3.02	0.79	41,063	0.004	2	95
Malaria risk map	**5**	**1**	**2.96**	**1.1**	**39,519**	**0.006**	**2**	**95**

high soil moisture. It is a swampy area with the presence of rice-growing lowlands due to the dense hydrographic network.

The low risk class covers 49.03% and occupies the north (Zuénoula health district), the center (Tibiéta, Bouafla, Angovia, Gbégbéssou, etc.), the rainfall in this zone is low and the temperatures are high (35˚C).

4.5. Validation of Risk Maps

Validation of the thematic maps was done by statistical analysis of the error or uncertainty associated with each map (Table 6). The uncertainties calculated on the malaria risk assessment factors vary from 0.002 to 0.006. Overall, the errors in the construction of these maps are minimal. The confidence level of the different malaria risk maps is significant (95%).

For the land use map, the uncertainty is 0.0003 or 3E−4 with a confidence interval of 68% which means that the land use map is not a good approximation of the areas at risk of these diseases.

5. Discussion

The use of Geographic Information Systems (GIS) and multi-criteria analysis in the Marahoué region resulted in the production of a climatic risk map, an environmental risk map and a land use map. The linear combination of these maps allowed the identification of potential malaria risk sites in this region in order to predict malaria infection and conduct effective malaria control.

The map of malaria risk due to climatic factors has a high risk of 48.36% to predict malaria in the Marahoué region. This risk is higher in the south, west, and northwest of the region. The south and west are characterized by abundant rainfall, temperatures ranging from 21˚C to 31.5˚C, and very high humidity (>75%). This result shows that heavy rainfall seems to predict malaria risk. According to Craig et al. (1999) a minimum of 80 mm of rainfall over a consecutive four-month period with average temperatures is essential for malaria transmission. Heavy rainfall results in the formation of temporary or permanent pools and puddles that are breeding grounds for mosquito larvae and abundant vector populations. According to Zhao et al. (2020), a weekly rainfall of more than 10 mm leads to the development of mosquitoes. The high humidity associated with it, favors mosquito survival (Gouataine & Ymba, 2018). Rainfall affects mosquito dynamics (Ndiaye et al., 2006) and increases the daily entomological inoculation rate of the vector (Dolo et al., 2003). They account for 60% of malaria anomalies (Niangaly, 2009). The risk due to environmental or ecological factors is dominated by a high degree of risk. This environmental risk is more marked in the south of the region and covers 55.29% of the area. This high risk is due to the high chlorophyll density (NDVI), high soil moisture (NDWI) reflecting the presence of swampy areas, low altitudes and the presence of water points. This result shows that NDVI, NDWI, altitude and water points predict malaria risk. This result confirms the work of Ferrão et al. (2021) carried out in the village of Sussundenga in Mozambique which states that human modified landscapes are conducive to malaria vectors. This result is very important because it shows that the Tasselrd-cap transformation generally used to study phenomena related to the environment is a technique that can be used in epidemiology. Studies by Martiny et al. (2012) in Bancoumana (Mali) have shown that NDVI can be used as an indicator of rainfall when rainfall data are lacking. Malaria transmission is accelerated, when the NDVI value exceeds the threshold of 0.36. These studies show that there is a 15-day lag between the increase in NDVI and the increase in malaria incidence, which is explained by the duration of the development of Anopheles larvae. With respect to altitude, the results show that this parameter influences the risk of malaria (Sahondra et al., 2001). Water points and market gardening areas maintain moisture for vector survival and transmission even in dry season (Martiny et al., 2012; Ferrão et al., 2021). This risk could be due to land use types (Ferrão et al., 2021). Indeed, the land use map shows that more than half of the region is occupied by crops and fallow. The southern part of the region, identified as a high-risk area, is dominated by food crops such as rice cultivation in the lowlands. These crops influence the distribution of malaria and therefore constitute risk factors (Dossou-Yovo et al., 1998). The annual cycle of vector abundance is linked to the variation in rainfall patterns and rice cultivation phases (Ravoahangimalala et al., 2003). And the density of vector aggressiveness is very high after the pricking of young rice shoots (Dossou-Yovo et al., 1998). Rainfall, relative humidity, temperatures (min and max), elevation, NDVI, NDWI, population density, land use, and distance to permanent water points are significant variables in predicting malaria risk (Dansou & Odoulami, 2015; Ferrão et al., 2021; Zewga, 2021). This method prioritizes malaria control based on climate, remote sensing, and mapping data. The distribution of the study area showed that 50.70% of the total area belongs to the high risk class and 49.03% to low risk. This indicates that the Marahoué region appears to be endemic for malaria. The calculation of uncertainties and confidence level shows that the proposed model for malaria prediction classifies well the risk areas with a good accuracy. The uncertainties are low and the confidence level of 95% gives a high reliability of the maps and allows the model to be used validly. These low uncertainties could be due to the fact that these parameters come from sources that have already been validated and are therefore more reliable. The climatic and environmental data (remote sensing data) introduced in the GIS allowed the prioritization of malaria risk areas.

6. Conclusion

Modelling using the multi-criteria analysis combination method was used to establish malaria risk maps, identified in two classes: the low risk class and the high risk class. The approach adopted in this work uses both climatic and environmental data. This approach has many advantages as it has contributed to the identification of malaria vulnerable areas for malaria prediction and rational decision making. However, these methods have limitations because the estimation of the parameters often lacks precision due to insufficient or completely missing data in some parts of the study area. Thus, sufficient data (health, climatic and environmental) should be available for the entire region to better determine all the risk factors for the spread of malaria in the region. Also, this methodological approach and the tools could be used at the national level for an effective fight against this pathology throughout the country. GIS remains an invaluable contribution to human health management.

Acknowledgements

The authors think the National Meterology (SODEXAM) for rainfall data, temperature minimum and maximum data and relative humidity data acquisition.

Author Contribution

Gouzile Assikohon Pulchérie, Bama Martial Zamina Bi Yourou Guillaume and developed the ideas and wrote the article with the contribution of Tiembre Issaka. Tié Albert Goula Bi and Soro Gneneyougo Emile supervised the paper. Yapi Ellélé Aimé contributed to the acquisition of data.

Conflicts of Interest

The authors declare no conflict of interest.

References

Beale, L., Abellan, J. J., Hodgson, S., & Jarup, L. (2008). Methodologic Issues and Approaches to Spatial Epidemiology. *Environmental Health Perspectives, 116,* 1105-1110. https://doi.org/10.1289/ehp.10816

Craig, M. H., Snow, R. W., & Le Sueur, D. A. (1999). Climate-Based Distribution Model of Malaria Transmission in Sub-Saharan Africa. *Parasitology Today, 15,* 105-111. https://doi.org/10.1016/S0169-4758(99)01396-4

Dansou, B. S., & Odoulami, L. (2015). Paramètres climatiques et occurrence du paludisme dans la commune de Pobè, au sud-est du bénin. In *XXVIIIe Colloque de l'Association Internationale de Climatologie* (pp. 129-132).

Diomandé, B. I., Coulibaly, K. A., & Soumahoro, S. P. (2017). Variabilité climatique et recrudescence du paludisme a Niangon dans la commune de Yopougon-Abidjan (Côte d'ivoire). *Revue Ivoirienne de Géographie des Savanes, 3,* 89-106.

https://docplayer.fr/88359004-Variabilite-climatique-et-recrudescence-du-paludisme-a-niangon-dans-la-commune-de-yopougon-abidjan-cote-d-ivoire.html

Dolo, A., Camara, F., Poudiougo, B., Touré, A., Kouriba, B., Bagayogo, M., Sangaré, D., Diallo, M., Bosman, A., Modiano, D., Touré, Y. T., & Doumbo, O. (2003). Épidémiologie du paludisme dans un village de savane soudanienne du Mali (Bancoumana): Étude entomo-parasitologique et clinique. *Santé Publique, 2319,* 308-312.

Dossou-Yovo, J., Ouattara, A., Doannio, J. M. C. et al. (1998). Enquêtes paludométriques en zone de savane humide de Côte d'Ivoire. *Médecine Tropicale, 58,* 51-56.

Eholié, S. P., Ehui, E., Adou-Bryn, K., Kouamé, K. E., Tanon, A., Kakou, A., Bissagnené, E., & Kadio, A. (2004). Paludisme grave de l'adulte autochtone à Abidjan (Côte d'Ivoire). *Santé Publique Bulletin de la Société de Pathologie Exotique, 97,* 340-344.

Ferrão, J. L., Earland, D., Novela, A., Mendes, R., Ballat, M. F., Tungaza, A., & Searle, K. M. (2021). Mapping Risk of Malaria as a Function of Anthropic and Environmental Conditions in Sussundenga Village, Mozambique. *International Journal of Environmental Research and Public Health, 18,* 2568.
https://doi.org/10.3390/ijerph18052568

Fosah, S., Mbouna, A. D., Efon, E., Achu, D. F., Andre, L., & Dikande, A. M. (2022). Influences of Rainfall and Temperature on Malaria Endemicity in Cameroon: Emphasis on Bonaberi District. *Journal of Geoscience and Environment Protection, 10,* 46-66.
https://doi.org/10.4236/gep.2022.103004

Gething, P. W., Boeckel, T. P. V., Smith, D. L., Guerra, C. A., Patil, A. P., Snow, R. W., & Hay, S. I. (2011). Modelling the Global Constraints of Temperature on Transmission of *Plasmodium falciparum* and *P. vivax*. *Parasites & Vectors, 4,* 92.
https://doi.org/10.1186/1756-3305-4-92

Gouataine, S. R., & Ymba, M. (2018). Variabilité climatique et émergence du paludisme a Bongor (Tchad). *Revue Espace, Territoires, Sociétés et Santé, 1,* 143-156.
https://retssa-ci.com/index.php?page=detail&k=40

Gramado, S., Ettien-Ablan, A. M., N'Gronma, N. A. B., Yao, K. A., Tanner, M., & Obrist, B. (2006). La vulnérabilité des citadins à Abidjan en relation avec le paludisme: Les risques environnementaux et la monnayabilité agissant à travers le palu sur la vulnérabilité urbaine. *Vertigo, 1767,* 13. https://doi.org/10.4000/vertigo.1767

Guerra, C. A., Gikandi, P. W., Tatem, A. J., Noor, A. M., Smith, D. L., Hay, S. I., & Snow, R. W. (2008). The Limits and Intensity of *Plasmodium falciparum* Transmission: Implications for Malaria Control and Elimination Worldwide. *PLOS Medicine, 5,* 300-311.
https://doi.org/10.1371/journal.pmed.0050038

Hay, S. I., Guerra, C. A., Gething, P. W., Patil, A. P., Tatem, A. J., Noor, A. M., Kabaria, C. W., Manh, B. H., Elyazar, I. R. F., Brooker, S., Smith, D. L., Moyeed, R. A., & Snow, R. W. (2009). A World Malaria Map: *Plasmodium falciparum* Endemicity in 2007. *PLOS Medicine, 6,* 1-18. https://doi.org/10.1371/journal.pmed.1000048

Joperin, F. (1995). Méthode multicritère d'aide à la décision et SIG pour la recherche d'un site. *Revue internationale de géomatique, 5,* 37-51.

Jourda, J. P., Saley, M. B., Djagoua, E. V., Kouamé, K. J., Biemi, J., & Razack, M. (2006). Utilisation des données ETM+ de Landsat et d'un SIG pour l'évaluation du potentiel en eau souterraine dans le milieu fissuré précambrien de la région de Korhogo (nord de la Côte d'Ivoire): Approche par analyse multicritère et test de validation. *Revue de Télédétection, 5,* 339-357.

Konan, Y. L., Koné, A. B., Doannio, J. M. C., Fofana, D., & Odehouri-Koudou, P. (2009). Transmission du paludisme à Tiassalékro, village de riziculture irriguée situé en zone sud forestière de Côte d'Ivoire. *Bulletin de la Société de pathologie exotique, 102,* 26-30.

Kotchi, S. O., Bouchard, C., Ludwig, A., Rees, E. E., & Brazeau, S. (2019). Utilisation des images d'observation de la terre pour améliorer la cartographie des risques de maladies associées au changement climatiques. *Relevé des maladies transmissibles au Canada, 45,* 148-158. https://doi.org/10.14745/ccdr.v45i05a04f

Kouame, A. K. D., Fofana, K. E. M., Mobio, A. B. H., Kassi, A. J.-B., Kouame, K. F., & Djagoua EM'moi, V. (2017). Cartographie De La Sensibilite Aux Maladies Environnementales Respiratoires Dans Le District Sanitaire De Koumassi-Port-Bouët-Vridi (Sud De La Côte d'Ivoire). *European Scientific Journal, 13,* 202. https://doi.org/10.19044/esj.2017.v13n5p202

Kouamé, A. K. D., Mobio, A. B. H., Djagoua, E. M. V., Affian, K., & Pottier, P. (2011). *Cartographie du risque bilharzienne à partir de l'utilisation combinée de la télédétection et du système d'information géographique* (18 p.).

Koudou, A., Adiaffi, B., Assoma, T. V., Sombo, A. P., Amani, E. M. E., & Biemi, J. (2013). Conception d'un outil d'aide à la décision pour la prospection des eaux souterraines en zone de socle du sud-est de la Côte d'Ivoire. *Geo-Eco-Trop, 37,* 211-226.

Martiny, N., Dessay, N., Yaka, P., Toure, O., Sultan, B., Rebaudet, S., Broutin, H., Piarroux, R., Chiapello, I., Sagara, I., Fontaine, B., Sissoko, M., Jeanne, I., Doumbo, O., & Gaudart, J. (2012). Le climat, un facteur de risque pour la santé en Afrique de l'ouest. *La meteorology,* No. Spécial AMMA, 73-79. https://doi.org/10.4267/2042/48135

Meyer-Waarden, L., & Zeitoun, H. (2005). Une comparaison empirique de la validité prédictive de la méthode de composition, de l'analyse conjointe et de l'analyse conjointe hybride. *Recherche et applications en marketing, 20,* 39-58. https://doi.org/10.1177/076737010502000304

Morjani, Z. (2003). *Conception d'un système d'information à référence spatiale pour la gestion environnementale, application à la sélection de sites potentiels de stockage de déchets ménagers et industriels en région semi-aride (Souss, Maroc)* (300 p.). Thèse de Doctorat, Université de Genève.

Ndiaye, P. I., Bicouta, D. J., Mondetb, B., & Sabatiera, P. (2006). Rainfall Triggered Dynamics of Aedes Mosquito Aggressiveness. *Journal of Theoretical Biology, 243,* 222-229. https://doi.org/10.1016/j.jtbi.2006.06.005

Niangaly, H. (2009). *Epidémiologie du paludisme dans le village de la plaine du pays dogon du Mali: Pongonon* (129 p.). Thèse de médecine à l'université de Bamako.

Oluwafemi, J., Babalola, S. O., Mukaila, I. O., & Badewa, A. O. (2022). GIS-Based Approach to Risk Mapping of Lassa Fever Outbreak in Akure South Local Government Area, Nigeria. *The International Archives of the Photogrammetry, Remote Sensing and Spatial Information Sciences, XLVI-4/W3-2021,* 147-153. https://creativecommons.org/licenses/by/4.0

PNLP (Programme National de lutte contre le paludisme). *Plan national de suivi et évaluation de la lutte contre le paludisme 2021-2025* (84 p.).

Rapport Annuel sur la Situation Sanitaire (RASS) 2018 édition 2019 (407 p.).

Ravoahangimalala, R. O., Rakotoarivony, H. L., Le Goff, G., & Fontenille, D. (2003). Écoéthologie des vecteurs et transmission du paludisme dans la région rizicole de basse altitude de Mandritsara, Madagascar. Entomologie médicale. *Le Bulletin de la Société de Pathologie Exotique, 96,* 323-328.

Saaty, T. L. (1977). A Scaling Method for Priorities in Hierarchical Structures. *Journal of Mathematical Psychology, 15,* 234-281. https://doi.org/10.1016/0022-2496(77)90033-5

Sahondra Harisoa, L. J., Pietra, V., Tombo, M. L., Albonico, M., Ranaivo, L. H., De Giorgi, F., Razanakolona, J., D'Ancona, F. P., Sabatinelli, G., Raveloson, A., Modiano, D., & Rakotondramarina, D. (2001). Système de surveillance épidémiologique et d'alerte du paludisme sur les Hautes Terres Centrales de Madagascar: Résultats 1999-2000. *Archives de l'Institut Pasteur de Madagascar, 67,* 21-26.

Saley, M. B. (2003). *Système d'information hydrogéologique à référence spatiale, discontinuité pseudo-image et cartographie thématique des ressources en eau de la région semi-montagneuse de Man (Ouest de la Côte d'Ivoire)* (209 p.). Thèse de Doctorat, Université de Cocody.

Somé, Y. C. S. (2010). *Modélisation de la distribution spatiale des formes moleculaires M et S d'Anophèles ganbiae Sensu Stricto au Burkina Faso avec les SIG et l'analyse spatiale* (309 p.). Thèse de doctorat à l'université d'Orléans: Spécialité, Géographie-Aménagement-Environnement.

WHO (2021). World Malaria Report 2021. Key Messages Information Pack, 24 p.

Yao, A. B., Goula, B. T. A., Kane, A., Mangoua, O. M. J., & Kouassi, K. A. (2014). Cartographie du potentiel en eau souterraine du bassin versant de la Lobo (Centre-Ouest, Côte d'Ivoire): Approche par analyse multicritère. *Hydrological Sciences Journal, 61,* 856-867.

Zewga, M. (2021). GIS Based Malaria Risk Assessment. *Health Science Journal, 15,* 7.

Zhao, X., Thanapongtharm, W., Lawawirojwong, S., Wei, C., Tang, Y., Zhou, Y., Sun, X., Cui, L., Sattabongkot, J., & Kaewkungwal, J. (2020). Malaria Risk Map Using Spatial Multi-Criteria Decision Analysis along Yunnan Border during the Pre-Elimination Period. *American Journal of Tropical Medicine and Hygiene, 103,* 793-809. https://doi.org/10.4269/ajtmh.19-0854